Journal of Ceramic Processing Research. Vol. 8, No. 2, pp. 156~160 (2007)

JOURNAL OF
Ceramic
Processing Research

Electrical properties of Sol-infiltrated PCW-PZT thick films on SiC thick films

Ki-Yong Choi[a,b], Duck-Kyun Choi[a] and Tae-Song Kim[b,*]

[a]*Division of Advanced Materials Science, 17 Hangdang-Dong, Seongdong-Gu, Hanyang University Seoul 133-791, Korea*
[b]*Nano-Bio Research Center, KIST, 39-1 Haweolgog-dong, Seongbuk-gu, Seoul 136-791, Korea*

We have fabricated a PCW-PZT thick film on Pt/TiO_2/SiN_x/SiC/Si substrates. SiC thick films were deposited on the Si substrate by a thermal CVD method. SiN_x films with different film thicknesses as a diffusion barrier layer were deposited on SiC/Si substrates using plasma enhanced chemical vapor deposition (PECVD). For application of a cantilever-based device, a SiC thick film was used as a supporting material in order to improve sensitivity of the cantilever-based sensor. A screen printed thick film and a sol infiltrated thick film were also compared. The PCW-PZT thick film showed a much denser microstructure using the sol infiltration method. The electrical properties of the PZT solid solution prepared were predominantly realized in the low temperature region. In the case of the sol infiltrated PCW-PZT thick film sintered at 850 °C, the remanent polarization (P_r) was about 12.7 μC/cm^2 at an applied field of 150 kV/cm, and the dielectric permittivity (ε_r) was 516 at a frequency of 100 kHz.

Key words: piezoelectric, MEMS, SiC, PZT, thick film, sol.

Introduction

The use of piezoelectric materials on micromachined silicon structures is of particular interest in the field of microelectromechanical systems (MEMS) [1]. Lead zirconate titanate (PZT) thick films have been widely used for the actuation of active structures in MEMS. The piezoelectric properties of such films with a thickness range of 5-50 μm make them suited to integrated actuation applications. For these applications, a candidate method for fabricating thick films is the screen printing method. However, the properties of screen printed thick films on Si-based substrates are poorer than those of bulk ceramics, due to some reaction between the PZT thick film and the Si-based substrate, and lower sinterability originating from the clamping effects of the substrate. The ability to produce high-quality (especially high density) piezoelectric thick films at a relatively low temperature is important in manufacturing useful piezoelectric actuators on Si substrates.

Also, in recent years, silicon carbide has emerged as an important material for MEMS applications [2, 3]. SiC is a wide band-gap semiconductor material which has a high-temperature stability, a high thermal conductivity, a high breakdown electric field, and a high electron saturation velocity, making it suitable for use in harsh environments [4-6]. The progress of 3C-SiC deposition onto various large area substrates [7] and the development of surface micromachining techniques for the fabrication of SiC devices [8, 9] in recent years had stimulated the use of SiC as a structural material for MEMS. Due to its high Young's modulus and relatively low mass density, SiC resonant structures can present much higher resonant frequencies compared to Si or GaAs structures with the same dimension [10].

PCW-PZT thick films with a SiC supporting layer have been developed in our laboratory. In the case of piezoelectric micro-cantilever sensors, Si has been used as the supporting material. However, in order to improve sensitivity in the sensor, it is necessary to use a high elastic modulus material. Because SiC has a higher elastic modulus than Si, it is desirable that as the supporting material of the cantilever. In order to use SiC thick films, a systematic study of the interfaces between PZT and SiC thick films, and SiC thick films and the bottom electrodes are needed, because of the technical importance for successful MEMS device applications. In a previous study [11], we used TiO_2 and SiN_x as the adhesion layer and diffusion barrier layer. Also, we have fabricated PZT thick films by sol infiltration in order to enhance the densification of the films. The sol infiltration was performed on a PZT printed wafer. In this study, we have fabricated PZT thick films treated with a diol-based sol to improve the performance of thick films, low temperature sinterable PZT powder was used, and sol infiltration was introduced after the screen printing. Therefore, in this study, we focused on the property improvement of the PCW-PZT thick film. A screen printed thick film and a sol infiltrated thick film were also compared.

*Corresponding author:
Tel : +82-2-958-5458
Fax: +82-2-958-6910
E-mail: tskim@kist.re.kr

Experimental Procedures

In a previous paper [12], the preparation and characterization of PZT (52/48)+0.12 mol% PCW thick films prepared by screen printing have been described. Figure 1 shows a schematic diagram of the multilayer structure that consists of a ferroelectric thick film, an electrode (Pt), an adhesion layer (TiO_2), a diffusion barrier layer (SiN_x) and the supporting material (SiC). A SiC thick film was deposited on the Si substrate by a thermal CVD method at a pressure of 10 Torr (1333 Pa) at 1000 °C. MTS (methyltrichlorosilane; CH_3SiCl_3) and H_2 were used as precursor materials. TiO_2 thin films 300 Å thick as an adhesion layer between the SiN_x and Pt were deposited by RF magnetron sputtering. A Pt film 3000 Å thick as the bottom electrode was deposited by RF magnetron sputtering. Also, in order to prevent the reaction between PZT and the SiC thick film, we used SiN_x as a diffusion barrier layer between the adhesion layer and the SiC thick film. SiN_x films with different thicknesses (3000 and 6000 Å) were deposited on SiC thick films using PECVD. Figure 2 shows the fabrication process of the PZT thick film and the sol infiltration. PCW-PZT paste was printed on the substrate using screen printing. Multiple printings and dryings were carried out up to 30 μm in final film thickness. The organic binder was burned out at 400 °C for 10 minute. Finally, all samples were sintered at a temperature between 750 and 950 °C for 10 minute. A Pt film 1500 Å thick as the top electrode was deposited by RF magnetron sputtering. In order to perform sol infiltration, a diol-based PZT sol was used. Firstly, a diol sol was poured onto the PZT printed wafer, which was executed after the process in which the organics were burned out at 400 °C. Subsequently, in order to increase the effect of the sol infiltration, an autoclave was filled with N_2 gas for 10 minute. After spinning to disperse the residue sol, the wafer was heated at 400 °C for 5 minute on a hot plate, and was then wafer heated at 650 °C for 10 minute in an electrical furnace to burn out the organics. This entire process of sol infiltration was performed three times. Thereafter PZT thick films were sintered at 750-950 °C.

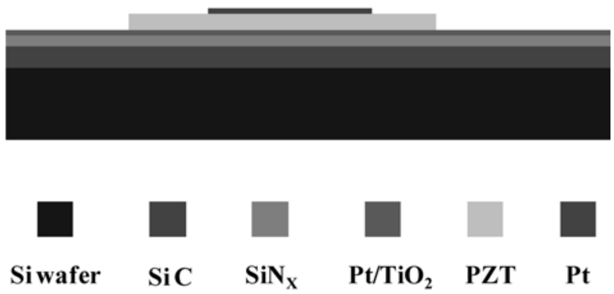

Fig. 1. A schematic diagram of the multilayer structure with a diffusion barrier layer (SiN_x).

The electrical properties such as remanent polarization (P_r), dielectric constant (ε_r), and tan δ were measured as a function of heat treatment temperature. The dielectric constant and the loss tangent were measured by an HP 4924A LF impedance analyzer at 100 kHz. The ferroelectric hysteresis behavior of the thick film can also be obtained using a RT66A ferroelectric tester-high voltage system (Radient technology Inc) with a virtual ground at applied fields of 150 kV/cm. In

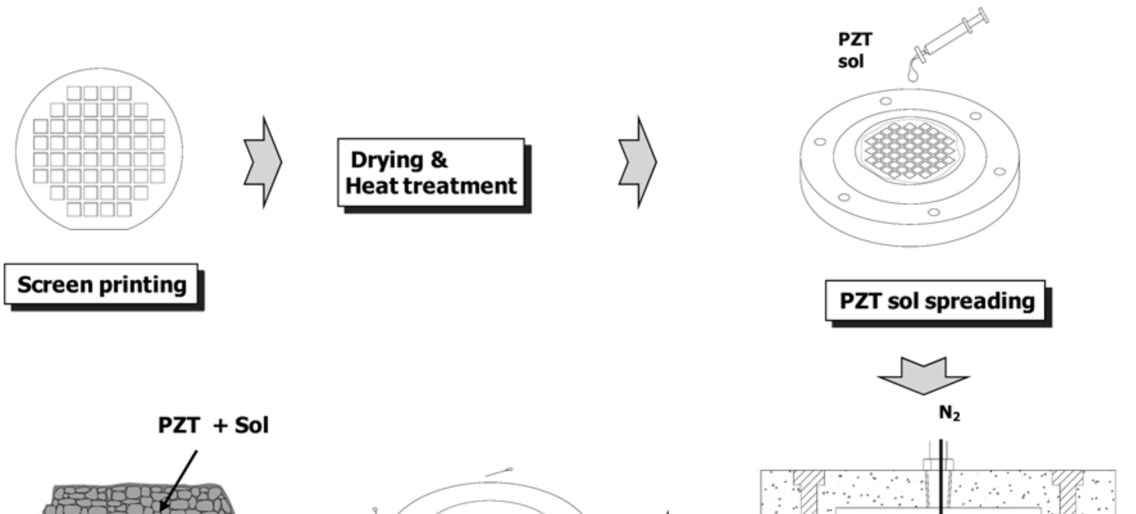

Fig. 2. Schematic drawing for the preparation process of a PCW-PZT thick film and sol infiltration.

addition, the interface between the PCW-PZT thick film and the SiC thick film were investigated using field emission scanning electron microscope (FE-SEM, Hitachi Co.).

Results and Discussion

In order to analyze the crystallographic orientation of the fabricated SiC thick film, X-ray diffraction (XRD) analysis was conducted. Figure 3 shows the XRD pattern of the SiC film deposited by a thermal CVD method on a Si substrate. Two peaks at $2\theta = 35.68°$ and $69.2°$ were observed. The peak at $2\theta = 69.2°$ is a Si substrate diffraction peak [13]. The peak at $2\theta = 35.68°$ corresponds to the 3C-SiC (111) orientation, indicating that the SiC thick film has a (111) preferred alignment. Figure 4(a) and (b) show SEM images of the cross-sections of PCW-PZT thick films after treatment at various sintering temperatures. As the sintering temperature increases, the sinterability was enhanced in the case of both the screen printed PCW-PZT thick films and the sol infiltrated PCW-PZT thick films. In a comparison with the screen printed PCW-PZT thick films, the sol infiltrated

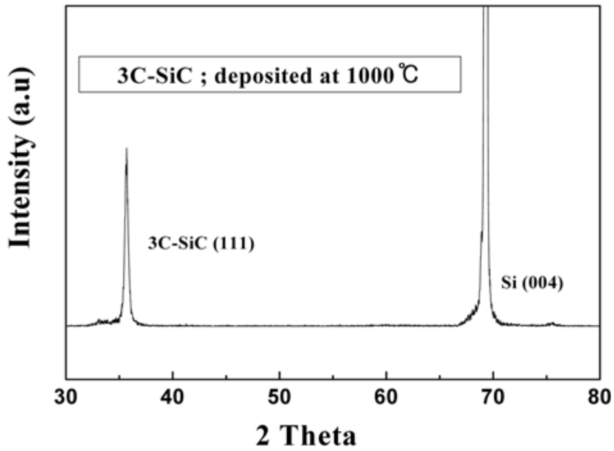

Fig. 3. XRD pattern of a SiC thick film deposited by a thermal CVD method on a Si substrate.

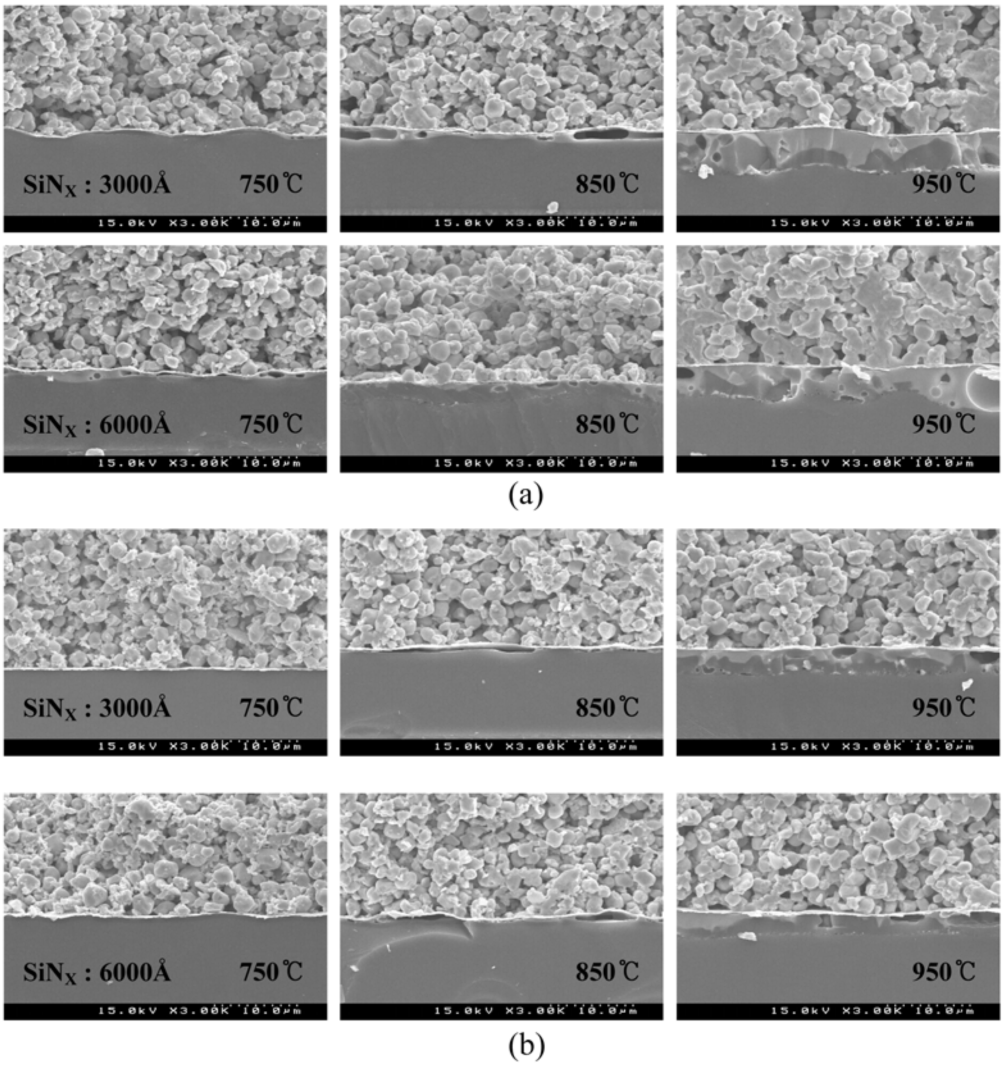

Fig. 4. SEM images of the cross-sections of PCW-PZT thick films for various sintering temperatures and SiN_X thicknesses: (a) printed only, (b) 3times infiltrated with diol sol.

Table 1. The dielectric constants and the loss tangents of the PCW-PZT thick films with different SiN_X thicknesses at various sintering temperatures

Temp. (°C)	Nomal treatment						sol treatment			
	0 Å		3000 Å		6000 Å		3000 Å		6000 Å	
	ε_r	Tan δ	ε_r	Tan δ	ε_r	Tan δ	ε_r	Tan δ	ε_r	Tan δ
750	274	0.029	208	0.028	242	0.024	453	0.042	452	0.04
800	317	0.031	312	0.03	317	0.026	459	0.042	482	0.04
850	358	0.032	330	0.033	412	0.031	502	0.047	516	0.041
900	408	0.036	429	0.033	456	0.033	532	0.052	568	0.042
950	308	0.025	572	0.035	551	0.044	516	0.036	513	0.039

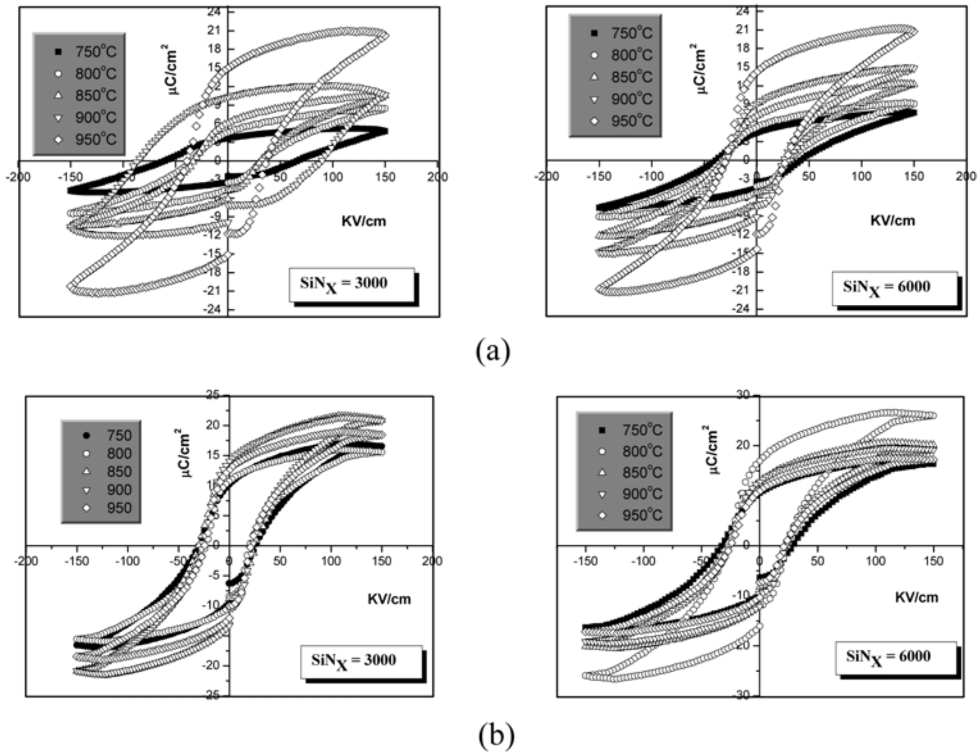

Fig. 5. P-E hysteresis curves of the PCW-PZT thick films treated at various sintering temperatures at a thicknesses of 3000 and 6000 Å: (a) screen printing only, (b) sol treated.

PCW-PZT thick films showed a more stable interface below 850 °C. However, SiC thick films, sintered at 900 °C and 950 °C, was found to partially change. The upper layer of SiC thick films partially reacted with Pb and O, as has been demonstrated using EPMA data [11]. SiN_x films as a diffusion barrier layer were deposited on the SiC/Si substrates in order to prevent the structural degradation of SiC due to the inter-diffusion and the reaction. Figure 4 shows that cross-section of the PCW-PZT thick films do not depend on SiN_x film thickness, or on the SiN_x films used as barrier layers. Densification of films is advantageous for the enhancement of the electrical properties of the thick films. The dielectric constants and loss tangents of the PCW-PZT thick films as a function of the sintering temperature are shown in Table 1. The dielectric constants of the PCW-PZT thick films increased with an increase in the sintering temperature. In order to further improve the microstructure and the electrical properties of thick films, a sol infiltration method was utilized to produce sol infiltrated thick films. The sol infiltrated thick films were fabricated through the thick film formation by screen printing in addition to the subsequent sol infiltration. The dielectric constants of the sol infiltrated thick films are larger than these of the screen printed thick films, indicating that the density of the sintered body can be increased by sol infiltration. From Figure 4(b), it is confirmed that the sol infiltrated thick films show a dense-microstructure with a relatively low amount of porosity. In addition, the piezoelectric properties of the sol infiltrated PZT thick films were highly enhanced due to the sol infiltration. Also, the dielectric constant of the thick films increased with a thickness increase of the diffusion barrier layer. The

Table 2. Remanent polarization of PCW-PZT thick films with different SiN_X thicknesses at various sintering temperatures at E_{max}=150 kV/cm

Temp. (°C)	Nomal treatment		sol treatment	
	3000 Å	6000 Å	3000 Å	6000 Å
750	4.2	4.4	10.2	10.5
800	5.2	5.2	10.7	16.4
850	6.5	6.1	13.3	12.7
900	10.2	8.6	14.0	12.7
950	15	13.0	12.6	10.9

loss tangent of PZT thick films was improved with a thickness increase of SiN_x diffusion barrier layer. From these results, it was found that the SiN_x with a thickness of around 6000 Å was more effective for the improvement of interfacial and electrical properties of PCW-PZT thick films. Figure 5 shows the P-E hysteresis loops of PCW-PZT thick films treated with screen printed (a) and sol infiltrated (b) thick film. And Table 2 show the remanent polarization (P_r) of PCW-PZT thick films as a function of the sintering temperature. The remanent polarization increased with an increase of sintering temperature in both screen printed and sol infiltrated thick films. Compared with the screen printed thick film, the sol infiltrated film showed a larger remanent polarization and dielectric constant. Concerning their microstructure, their electrical properties were affected by the difference of sinterability and densification between the screen printed thick film and the sol infiltrated thick film. The P-E hysteresis loops of the screen printed films show a soft type-shape, whereas the sol infiltrated thick films show a hard type-shape. It is evident that the PCW-PZT powder is suitable for low temperature sintering, sufficient to be compatible with silicon micromachining technology. Accordingly, it is concluded that the thick film prepared using the PZT-PCW powder can be adapted for use with piezoelectric micro-devices based on a silicon substrate, as it shows a very well-developed dielectric constant and P-E hysteresis loop. In case of the PCW-PZT thick films sintered at 850 °C, the remanent polarization (P_r) at a sweep electric field of ± 150 kV/cm was 12.7 μC/cm^2, and the dielectric constant was 516 at a frequency of 100 kHz.

Conclusions

We have fabricated the PCW-PZT thick films treated by screen printing and sol infiltration methods. In this study, to improve the microstructure and electrical properties of PCW-PZT thick films, we made use of sol infiltration. A diol-based sol infiltration method was more effective for the improvement of the microstructure and electrical properties of the PCW-PZT thick film. The electrical properties of sol infiltrated PCW-PZT thick films improved with an increase of sintering temperature. The dielectric permittivity (ε_r) of PCW-PZT thick films, sintered at 850 °C, measured at a frequency of 100 kHz was 516. Also, the PCW-PZT thick films exhibited well-saturated hysteresis loops. The remanent polarization (P_r) of a PCW-PZT thick film, sintered at 850 °C, was 12.7 μC/cm^2 at a sweep electric field of ±150 kV/cm. The electrical properties of the thick films prepared are largely affected by their microstructure. It became clear that the PCW-PZT powder is suitable for low temperature sintering such that it is compatible with silicon micromachining technology. Consequently, this implies that the thick films prepared can be adapted for use with Si-based MEMS applications, which require a low temperature sintering.

Acknowledgements

The authors are grateful for the financial support by Intelligent Microsystem Center sponsored by Korea Ministry of Science and Technology as a part of the 21st century's Frontier R&D Projects (Grant MS-01-133-01).

References

1. I.H. Kim, S.H. Seok, H.C. Kim, M.K. Kang, and K.J. Chun, Journal of Semiconductor Technology and Science 6[4] (2006) 293-268.
2. M. Mehregany, and C.A. Zorman, Thin Solid Films 355/356 (1999) 518-524.
3. P.M. Sarro, Sen. Actuators A 82 (2002) 210-218.
4. S. Sriram, R.C. Clarke, A.A. Burk, Jr., H.M. Hobgood, P.G. McMullin, P.A. Orphanos, R.R. Siergiej, T.J. Smit, C.D. Brandt, M.C. Driver, and R.H. Hopkins, IEEE Electron Device Lett. 15 (1994) 458-459.
5. N. Susumu, A. Sadao, Jpn. J. Appl. Phys. 33 (1994) 1833-1834.
6. H. S. Kong, J.W. Palmour, J.T. Glass, and R.F. Davis, Appl. Phys. Lett. 51 (1987) 442-444.
7. C.A. Zorman, M. Mehregany, Silicon carbide for MEMS and NEMS –an overview, Proc. IEEE 2 (2002) 1109-1114.
8. L. Jiang, R. Cheung, M. Hassan, A.J. Harris, J.S. Burdess, C.A. Zorman, and M. Mehregany, J. Vac. Sci. Technol. B 21 (2003) 2998-3001.
9. L. Jiang, M. Hassan, R. Cheung, A.J. Harris, J.S. Burdess, C.A. Zorman, and M. Mehregany, Proceedings of the 30th international conference on micro and nano engineering (2005) 106-111.
10. Y.T. Yang, K.L. Ekinci, X.M. Huang, L.M. Schiavone, M.L. Roukes, C.A. Zorman, and M. Mehregany, Appl. Phys. Lett. 78 (2001) 162-164.
11. K.Y. Choi, D.K. Choi, J.Y. Park, D.S. Yoon, and T. S. Kim, Integrated Ferroelectric 69 (2005) 93-101.
12. Y.B. Kim, H.J. Kim, C.I. Cheon, D.J. Choi, and T.S. Kim, Integrated Ferroelectric 41 (2001) 107-116.
13. R.J. Iwanowski, K. Fronc, W. Paszkowicz, and M. Heinonen, J. Alloys & Compounds 286 (1999) 143-147.